

⁹For the Nb sample described in reference 4, C_{es} was apparently slightly larger than that of Nb II, but

the authors attributed the excess over the lattice heat capacity to strains or impurities.

F¹⁹ NUCLEAR MAGNETIC RESONANCE LINE NARROWING IN LaF₃ AT 300°K

Kenneth Lee and Arden Sher

Varian Associates, Palo Alto, California

(Received 17 May 1965)

The fluorine nuclear magnetic resonance (nmr) of a single crystal of lanthanum trifluoride, LaF₃, has been investigated at 16.00 Mc/sec in the temperature range from 173 to 573°K. The resonance line was observed to begin motionally narrowing at 300°K.^{1,2} This is surprising since the melting point of LaF₃ is 1770°K. The purpose of this paper is to report the details of this observation.

Figure 1 shows the integrated spectra taken at three different temperatures with the magnetic field along the *c* axis of this hexagonal crystal.³ Within the experimental accuracy the linewidth and line shape are the same along the *c* axis and perpendicular to the *c* axis. Below the 300°K the rigid-lattice line shape is squarer than a Gaussian. This is evident from Fig. 1. The measured ratio of the fourth moment to the second moment squared, $M_4/(M_2)^2$, for the rigid lattice is 2.3, which compares to 3.0 for Gaussian. As the temperature is raised above 300°K, the line narrows and becomes a composite of a broad and narrow line. In this temperature region the ratio $M_4/(M_2)^2$ reaches a peak value of 3.8. The frequencies of the two lines are shifted but never enough to be resolved by the Rayleigh criterion. As the temperature is raised still further, the two lines coalesce and the line stops narrowing.⁴ In this high-temperature region $M_4/(M_2)^2$ decreases to a constant value of 3.2.

The experimental measurements were performed on a Varian V-4200 nmr spectrometer operated at 16.00 Mc/sec. The temperature dependence was obtained using a Varian V-4540 variable temperature controller which controls and monitors the flow of cooled or heated dry nitrogen gas over the sample. The single crystal used was cylindrical with a diameter of $\frac{1}{4}$ in. and a length of $\frac{3}{8}$ in. In order to avoid distortions and saturation, the magnetic field scanning speed, the modulation frequency and amplitude, and the magnitude

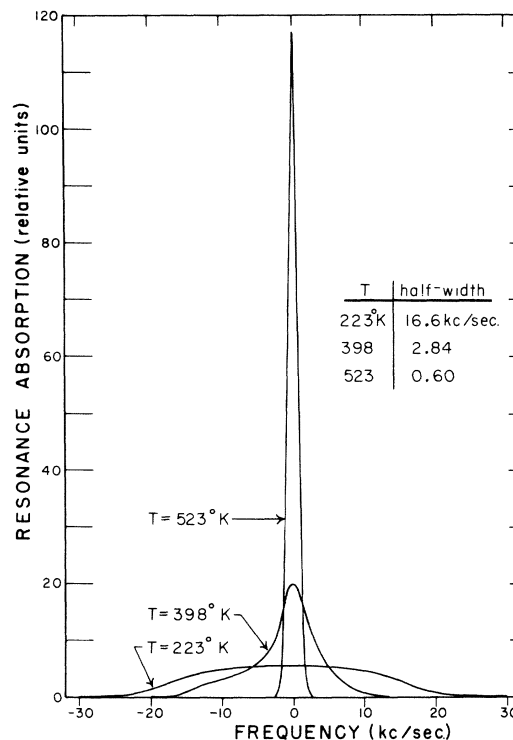


FIG. 1. Temperature dependence of F¹⁹ nmr absorption along the *c* axis. The half-width at half-intensity is given for the three temperatures.

of the rf field were chosen at each temperature such that by decreasing their magnitudes still further no changes in the resonance line were observed. The spectrum at each temperature was scanned as many as 100 times and stored in a C-1024 time-averaging computer. This procedure improves the signal-to-noise ratio as the square root of the number of scans. The use of this procedure was necessary because below 300°K the line is so broad that a signal-to-noise ratio of unity was typical for a single passage through the resonance line. However, at high temperatures, the signal-to-noise is greatly enhanced because of

the observed narrowing. The spectra were recorded as the derivatives of the absorption curves. The derivative data were then integrated on an IBM 7094 computer. M_2 and $M_4/(M_2)^2$ were also calculated by the IBM 7094.

Figure 2 is a plot of the half-width at half-intensity as a function of temperature along the two directions. The scatter in the low-temperature region is due to the relatively broad line which gives rise to a poor signal-to-noise ratio. The high-temperature linewidth of 1.2 kc/sec = 0.3 G is not limited by magnetic field inhomogeneities. Thermal-expansion measurements suggest that the motional narrowing is due to diffusion which arises from Schottky defect vacancies.⁵ The diffusion coefficient $D(T)$ varies exponentially as $D(T) = D_0 \exp[-E_A/(kT)]$, where D_0 is the diffusion coefficient at infinite temperature and E_A is the activation energy for diffusion. The measured E_A obtained from the slope of a semilog plot of the half-width as a function of $1/T$ is $E_A = 0.43 \pm 0.05$ eV. This E_A is much smaller than those generally found in solids. At the temperature T_N for the onset of narrowing, theory predicts $(M_2)^{1/2} \tau_C \cong 2\pi$, where τ_C is the correlation time. With $T_N \cong 300^\circ\text{K}$ and with the measured rigid-lattice root second moment $(M_2)^{1/2} = 10.6 \pm 0.2$ kc/sec, $\tau_C = 5.92 \times 10^{-4}$ sec is determined. Since $D(T_N) \cong a^2/(12\tau_C)$, where $a \cong 2.6$ Å is the average near-neighbor distance, a value $D_0 = (4.2 \pm 1.0) \times 10^{-4}$ cm²/sec is found.

The measured rigid-lattice root second moment of 10.6 kc/sec is in good agreement with

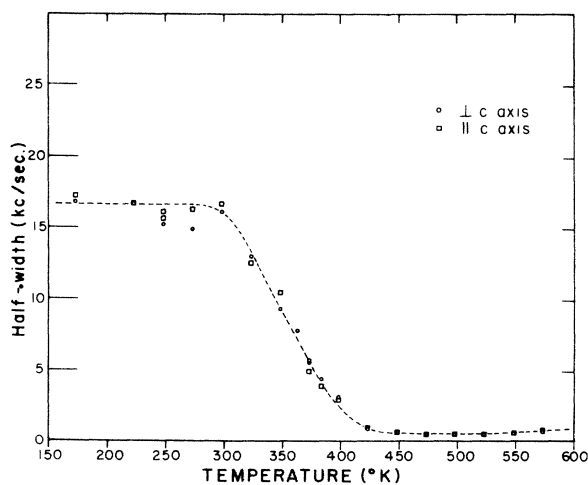


FIG. 2. Temperature dependence of F^{19} nmr half-width. The data are taken parallel and perpendicular to the c axis.

the second moments calculated from the Van Vleck expressions.² Taking into account the 60 nearest neighbors, these calculated values are 10.5 and 10.7 kc/sec for H_0 respectively parallel and perpendicular to the c axis. Although the exact crystal structure of LaF_3 is still in question,⁶ the data from Wyckoff,³ which indicate a hexagonal structure ($P6_3/mcm$) with three nonequivalent fluorine sites, was used in these calculations. There are effectively only two nonequivalent fluorine sites as far as the fluorine-fluorine magnetic dipole interactions are concerned. One site has twice as many fluorines as the other. The second moments for the spins on each of the two sites were calculated separately and then they were combined, assuming there was no frequency shift between the two sites. This is a reasonable assumption since the observed frequency shift is only about one-fifth of the rigid-lattice second moment.

The two lines observed at 398°K are not sufficiently well resolved to make accurate statements about their relative areas, widths, and frequency shift. The center frequency of the broad line was chosen to be halfway between the frequencies corresponding to one-twentieth of the intensities of the peak height. The broad line was then drawn as a best fit to the experimental curve, with the restriction that both the broad line and the residual narrow line be symmetric. The frequency shift is then found to be 3 kc/sec, the half-widths of the broad and narrow lines are 8.1 and 2.2 kc/sec, respectively, and the ratio of the area of the broad line to the narrow line (or the spin ratio) is 0.9. A frequency shift of this magnitude indicates the presence of some covalent bonding. The spin ratio contributing to the two lines (0.9) is in doubt because of the poor signal-to-noise ratio. In a 0.1% Gd-doped sample in which T_1 is smaller and the signal intensity correspondingly enhanced, the spin ratio was found to be approximately two. This ratio of two is in agreement with our assumption of two fluorine spins at one type of site and one fluorine spin at the other.

A detailed report on the results of both the pure and rare-earth-doped LaF_3 will be presented elsewhere.

We wish to thank H. Muir who grew the single crystals, and A. Wehlau and J. Shelley who performed the computer analysis of the data.

¹Kenneth Lee and Arden Sher, Bull. Am. Phys. Soc.

9, 733 (1964).

²See, for example, A. Abragam, The Principles of Nuclear Magnetism (Clarendon Press, Oxford, England, 1961).

³R. W. G. Wyckoff, Crystal Structures (Interscience Publishers, Inc., New York, 1964), Vol. 2.

⁴In fact, the line begins to broaden again at higher temperatures. This effect was first pointed out by M. Goldman and L. Shen who will publish more de-

tailed high-temperature data and an explanation of this effect.

⁵These measurements will be reported in detail elsewhere.

⁶D. A. Jones, J. M. Baker, and D. F. D. Pope, Proc. Roy. Soc. (London) 74, 249 (1959); R. A. Buchanan and H. H. Caspers, Naval Weapons Evaluation Facility Report No. 8213, 1964 (unpublished); W. M. Yen, W. C. Scott, and A. L. Schalow, Phys. Rev. 136, 271 (1964).

NONLINEAR OPTICAL REFLECTION FROM A METALLIC BOUNDARY*

Fielding Brown, Robert E. Parks, and Arthur M. Sleeper

Williams College, Williamstown, Massachusetts

(Received 3 May 1965)

Of the many nonlinear optical effects reported since Franken's discovery,¹ none has confirmed the generation of optical harmonics by a conduction electron plasma. Although Ducuing and Bloembergen² have studied harmonics generated by semiconducting mirrors, the observed effects are not related to the motion of conduction electrons, occurring only for noncentrosymmetric crystals and for power levels several orders of magnitude less than those here employed. The purpose of the present Letter is to report the unambiguous observation of second-harmonic light generated on reflection of a giant-pulse laser beam from the surface of a silver mirror. The present situation is distinct from earlier cases of optical harmonic generation, because the host lattice is centrosymmetric and the lack of symmetry of the reflecting boundary is responsible for the harmonic production. The observations are consistent with a second-harmonic polarization proportional to $\vec{E} \nabla \vec{E}$. Since only the component

of \vec{E} normal to the surface has a discontinuity at the boundary, the second-harmonic polarization would be proportional to $\cos^2\theta$, where θ is the angle between \vec{E} and the plane of incidence. The second-harmonic intensity would be proportional to $\cos^4\theta$.

Figure 1 describes the apparatus used to detect the effect and measure its angular dependence. The principal feature is the prism assembly consisting of three right-angle prisms with evaporated silver mirror surfaces mounted together as a unit. A ray incident on one side of the assembly then undergoes specular reflection at four successive surfaces and emerges in a direction colinear with the original beam. The arrangement permits both laser and monochromator to remain fixed, while θ can be varied by rotating the prism assembly around the beam as axis. The filter inserted after the third reflection eliminates harmonic light from all but the last surface and limits observed effects to those associated with reflection from a sin-

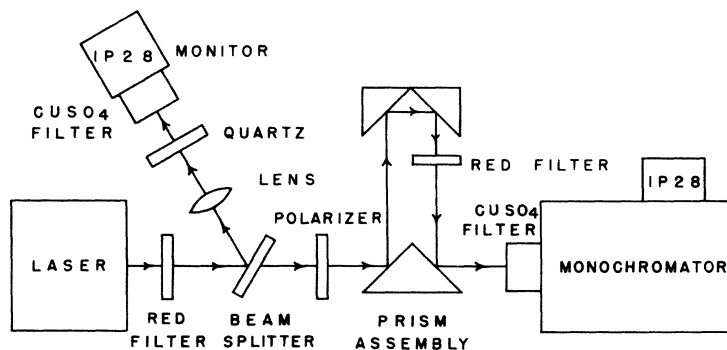


FIG. 1. Diagram of apparatus.